

ACCRETION DISK STRUCTURE AND BRANCH BEHAVIOR OF CYGNUS X-2

AKIRA HIRANO,¹ SHUNJI KITAMOTO,² AND TATSUYA T. YAMADA³

Department of Earth and Space Science, Faculty of Science, Osaka University, 1-1, Machikaneyama-cho, Toyonaka, Osaka 560, Japan

SHIN MINESHIGE⁴

Department of Astronomy, Faculty of Science, Kyoto University, Sakyo-ku, Kyoto 606-01, Japan

AND

JUN FUKUE⁵

Astronomical Institute, Osaka Kyoiku University, Kashiwara, Osaka 582, Japan

Received 1994 June 30; accepted 1994 December 16

ABSTRACT

A new analysis of the branch behavior of Cygnus X-2 is presented, applying a new disk model with a free parameter of a radial temperature gradient, $q = -d \log T / d \log r$, for the spectral fitting. We find that the spectral fitting is significantly improved for about one third of data and that the derived q -value changes from 0.67 to 0.85 in accordance with the spectral evolution from the horizontal branch (HB) to the flaring branch (FB) via the normal branch (NB). Two positive and negative correlations are found between the inner disk radius (R_{in}) and q , and between R_{in} and the inner disk temperature (T_{in}). Possible new interpretations regarding the branch behavior of Cyg X-2 are discussed based on these results.

Subject headings: accretion, accretion disks — stars: individual (Cygnus X-2) — X-rays: stars

1. INTRODUCTION

Low-mass X-ray binaries (LMXBs) are close binaries comprising a neutron star (or a black hole) and a late-type companion star. There has been long debate between two distinct interpretations as to the energy spectrum of LMXBs: One is proposed by Mitsuda et al. (1984) in which the spectrum is made up of two components: a multicolor blackbody spectrum emitted from an accretion disk and a blackbody spectrum from the surface of a neutron star. This model has been improved so as to incorporate the effects of Compton scattering by an accretion disk corona, thereby giving a better fit to the data (Mitsuda & Dotani 1989). Another interpretation is proposed by White, Peacock, & Taylor (1985), in which the X-ray spectrum is described by an unsaturated Comptonization (Sunyaev & Titarchuk 1980) of low-energy photons. History of the discussion and comparison between these two models have been reviewed by some authors (e.g., White, Stella, & Parmar 1988; Mitsuda & Dotani 1989; Kitamoto, Tsunemi, & Roussel-Dupre 1992). It is difficult to choose a better model in the above two from the energy spectral shape only, because of the smooth spectra. However, in this work, the model consisting of the multicolor blackbody spectrum and the blackbody spectrum is examined. The derived results must be helpful for further study on the X-ray emission mechanisms.

One possible key to understanding the emission mechanism of LMXBs resides in its temporal variation. Especially, the color-color-diagrams (CCD) and the hardness-intensity diagrams (HID) have often been used to describe time-dependent spectral evolution (e.g., Schultz, Hasinger, & Trümper 1989). Two classes of LMXBs are now distinguished, depending on

their distinct behavior in these diagrams. Bright sources generally trace a Z-shaped locus on the CCD or the HID (Hasinger 1987), therefore, they are called Z-sources (Hasinger & van der Klis 1989). The trajectories of X-ray bursters on the CCD or the HID are more complex and they are called atoll sources (Hasinger & van der Klis 1989).

This paper is concerned with the origin of the characteristic spectral behavior of Z-sources on the CCD and the HID. Theoretical efforts towards understanding the behavior of Z-sources have been made by Hoshi & Mitsuda (1991) and Hoshi & Asaoka (1993). They stood on the viewpoint by Mitsuda et al. (1984) and examined the time variations in the temperatures and the radii of the emitting areas both for the disk and the neutron-star components (see also You et al. 1992 for an alternative interpretation). We, however, point out here that, although the simple multicolor blackbody model originally proposed by Mitsuda et al. (1984) was frequently used to analyze Galactic X-ray sources and could provide a reasonable fit to the observed data before *Ginga* observations, more sophisticated models are now required to fit the statistically improved data by *Ginga* (e.g., Ebisawa, Mitsuda, & Hanawa 1991). With *Ginga* data, in fact, we can discuss possible deviations of the actual disk systems from the standard-model description (Shakura & Sunyaev 1973), and such deviations, we believe, might contain an important physics which plays a key role in the branch behavior of Z-sources.

Since it is difficult, at the present, to construct a new model which can totally replace the standard Shakura-Sunyaev model, we just relax one assumption of the standard model and require a radial effective temperature profile being prescribed as

$$T_{\text{eff}} \propto r^{-q}, \quad (1)$$

where r is a distance from the compact star, and q is a numerical constant to be determined from the spectral fitting.

In the original simple multicolor blackbody model, it is assumed that the effective temperature is proportional to $r^{-3/4}$,

¹ hirano@ntttd.nitt.jp.

² kitamoto@ess.sci.osaka-u.ac.jp.

³ yamada@vega.ess.sci.osaka-u.ac.jp.

⁴ minesige@kustastro.kyoto-u.ac.jp.

⁵ fukue@cc.osaka-kyoiku-u.ac.jp.

whereas the standard accretion disk model predicts that $T_{\text{eff}} \propto r^{-3/4} [1 - \beta(r_{\text{in}}/r)^{1/2}]^{1/4}$, where r_{in} is the innermost disk radius and β is a coefficient for the torque-free boundary condition. Therefore, we see $T_{\text{eff}} \propto r^{-3/4}$ only at $r \gg r_{\text{in}}$. The simple multicolor disk blackbody model is of limited use when discussing the X-ray spectral evolution, since about a half of X-rays are emitted within the radius of $10r_{\text{in}}$ from the compact object (Shakura & Sunyaev 1973). Hanawa (1989) proposed a more sophisticated model for the disk spectra, including the general relativistic effect without the above approximation. We have many other reasons, besides the general relativistic effect, to believe that a radial temperature gradient could deviate from the standard relation, $T_{\text{eff}} \propto r^{-3/4}$ (Honma & Mineshige 1993; Mineshige et al. 1994a, 1994b), for example; Irradiation by the central object (Czerny, Czerny, & Grindlay 1986; Sanbuchi, Yamada, & Fukue 1993); The presence of disk wind mass loss (Honma & Mineshige 1993); and the steady-state assumption postulated in the standard model may break down in the case of variable X-ray sources.

Cyg X-2 is one of the well-studied Z-sources. Its distance was reported to be 8 kpc (Cowley, Crampton, & Hutchings 1979). It was observed with the Large Area Proportional Counters (LAC) on-board *Ginga* (Turner et al. 1989) in 1988 June, as a part of a multiwavelength observing campaign with radio, UV, and optical wavelengths (Hasinger et al. 1990; Hjellming et al. 1990; van Paradijs et al. 1990; Vrtilik et al. 1990). During the observation runs, Cyg X-2 exhibited all three spectral states, the horizontal branch (HB), the normal branch (NB), and the flaring branch (FB), showing up the Z-shaped locus on the X-ray color-color diagram. All the informations, together with the results of the standard analysis, have been presented by Hasinger et al. (1990).

In the present study, we use the same data of Cyg X-2, but give new information concerning the accretion disk structure and the branch behavior on the basis of a more sophisticated description for the disk model; the radial-temperature-gradient-free model. The details of the observations will be summarized in § 2. We will then present our new fitting to the statistically best data observed by *Ginga* in § 3. We will see there the radial-temperature-gradient (q) to be variable in accordance with the spectral evolution, whereas q should be constant in the framework of the standard model. Furthermore, two positive and negative correlations are found between inner disk radius (R_{in}) and q and between R_{in} and inner disk temperature (T_{in}), respectively. Possible interpretations regarding the branch behavior are discussed on the basis of the radial-temperature-gradient-free disk model in § 4. The final section is devoted to conclusions.

2. OBSERVATION

Observations were carried out by the Large Area Proportional Counters (LAC) with a large effective area of 4000 cm² (Turner et al. 1989) on-board *Ginga* (Makino et al. 1987) in the interval from 1988 June 10 to June 14.

For the study of spectra, 48-channel pulse-height mode covering 1–37 keV were mainly used. Every 0.5 or 2s, a 48 channel pulse-height spectrum can be available. Others are observed with 12-channel pulse-height mode with 62.5 ms time resolution. Journal of the observation, light curves, the color-color diagram (CCD) and the hardness intensity diagram (HID) have been published by Hasinger et al. (1990). Typical three branches; the horizontal branch (HB), the normal branch (NB) and the flaring branch (FB), can be recognized.

In this work, because of low reliability of the collimator transmission response for the low transmission region, only the high collimator transmission (> 70%) data were used.

3. ANALYSIS AND RESULTS

Time sequence of X-ray energy spectra are accumulated for every ~10 minutes and 81 spectra with 48 channels were generated from all the observation. The new fitting including a temperature gradient (q) was performed for these 48-channel pulse height data. The analyzed energy range was restricted between 1.7 and 37.1 keV, and three energy channels below 1.7 keV were removed because of low reliability in the response function. The radial-temperature-gradient-free model can be formulated as

$$f(E) \propto \int_{T_{\text{out}}}^{T_{\text{in}}} \left(\frac{T}{T_{\text{in}}} \right)^{-2/q-1} B(E, T) \frac{dT}{T_{\text{in}}}, \quad (2)$$

where T_{in} and T_{out} are temperatures at the inner and outer edge of the disk, respectively, and $B(E, T)$ is the Planck function. Since the energy band used for the spectral fitting is restricted in the X-ray region, T_{out} is practically zero. Therefore, the fitting parameters are T_{in} , q and $R_{\text{in}}(\cos i)^{1/2}$ [$R_{\text{in}}(\cos i)^{1/2}$ is a proportional coefficient], where i is an inclination. We performed the spectral fitting by the two-component model similar to that of Mitsuda et al. (1984). One component is the disk model given by equation (2) and the other is a blackbody component given by a Planck function. Column density of interstellar neutral hydrogen is fixed to be $N_{\text{H}} = 10^{20}$ H atoms cm⁻². In the flaring branch and at a bottom of the normal branch, an Fe K-edge absorption feature with a column density of the order of 10^{19} cm⁻² is needed to get a reasonably good fitting. The Fe K-edge absorption feature has two parameters: the column density of the ionized Fe, which is left as the free parameter, and the K-edge energy which is fixed to be 8.0 keV.

The derived temperature should be interpreted to be a color temperature. The inner disk radius, $R_{\text{in}}(\cos i)^{1/2}$, is a tentative value calculated with assuming an effective temperature is equal to an obtained color temperature. Thus the derived values might be not the true radius and be underestimated values. (Ebisuzaki & Nakamura 1988; Kitamoto et al. 1992). On this calculation the distance to Cyg X-2 is assumed to be 8 kpc (Cowley et al. 1979).

Figure 1 plots in the HID the data points derived from each of the 48-channel spectral data. These data cover all the three branches. For the later convenience we reorder and number all the 48-channel spectral data according to the locus on the HID. Hereafter we call it the HID sequence number, N , which is also indicated in Figure 1. Although there is some ambiguity when determining the order around the lower-right part, minor changes in the order do not affect the results and the discussion.

The radial-temperature-gradient-free model significantly improves the fitting for about one-third of the spectra. Figure 2 shows three examples, in which the fitting by this new model and that by the conventional multicolor disk model are compared. The spectra are obtained (a) at the left end of the HB ($N = 1$), (b) at the apex between the HB and the NB ($N = 45$) and (c) around the bottom of the NB ($N = 66$). The upper panels show the observed spectra and best-fit model spectra by the new model: a soft component is a radial-temperature-gradient-free model and a hard component is a blackbody. The

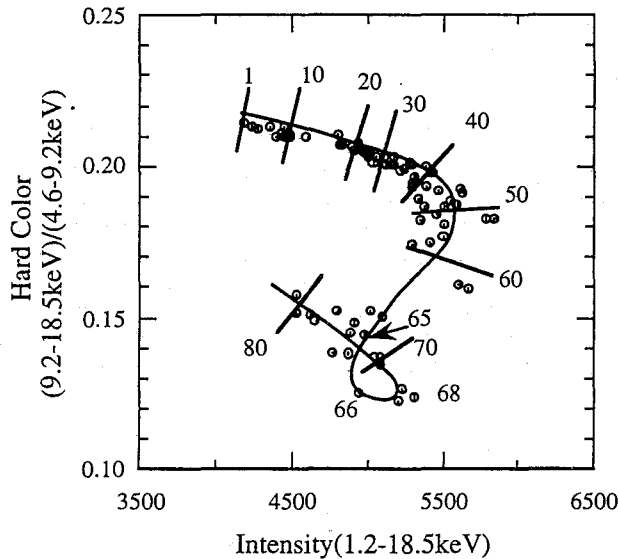


FIG. 1.—HID which is drawn by plotting the data points derived from each of the spectral data. The spectral data are recorded according to the locus of the HID (HID sequence number, N). N smaller than 50 constructed the horizontal branch (HB). The normal branch (NB) is from 50 to about 65. After 65, the data are contained within the flaring branch (FB).

middle and the lower panels plot the residuals from the best-fit conventional model and from the best-fit new model, respectively. Evidently this new model provides a better fit for the HB spectra. The statistical treatment using F -test will be described later.

In this fitting, the low-energy absorption, N_{H} , is fixed to be 10^{20} H atoms cm^{-2} . This value is so small comparing the effective absorption of the entrance window of the detector that the low-energy shape is almost independent on the N_{H} -value. Especially for the HB spectrum ($N = 1$), since the residuals to the $q = 0.75$ model indicate soft excess, even if N_{H} -value is kept to be a free parameter, no improvement of the fitting can be expected. For examples, the $\chi^2/\text{d.o.f.}$ values are 71.0/40, 39.5/40, and 95.5/39 for $N = 1$, $N = 45$, and $N = 66$, respectively. The figures show a small blackbody component at the bottom of the NB ($N = 66$) and best-fit q -value increases from the HB to the NB. The details of the parameters will be described later.

The inclusion of the new fitting parameter q does not simply mean minor modifications to the model at least for some cases. Rather, we need q to see structural changes in accordance with the branch transitions. Note that we do not include iron K lines in these fittings, since the iron line feature does not affect the fitting to the continuum spectra.

The fitting results are shown in Figure 3. The HID sequence number less than 50 corresponds to the data when Cyg X-2 was on the horizontal branch (HB). On the normal branch

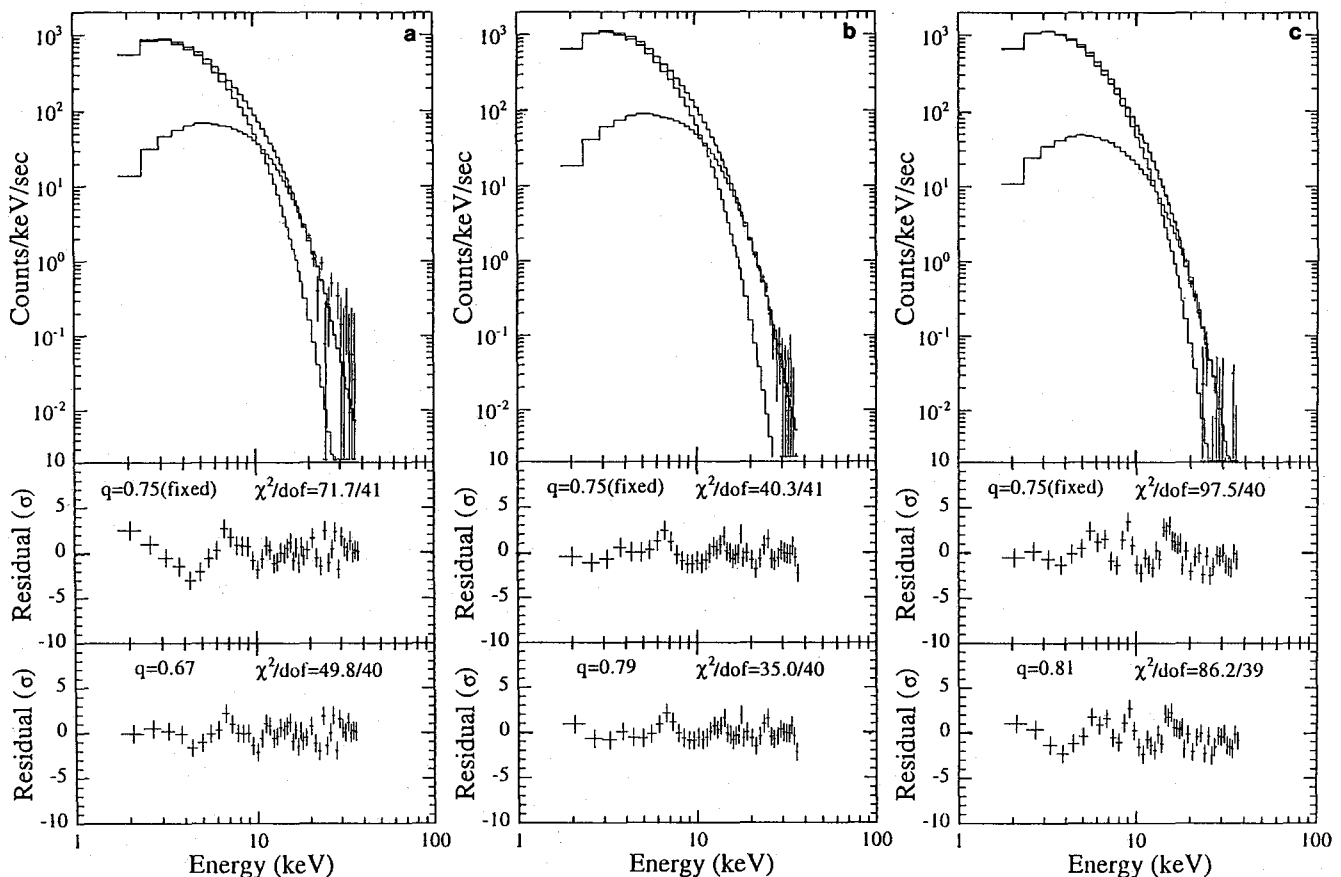


FIG. 2.—Three examples for a comparison between the fitting by the new model and by the conventional multicolor disk model. The spectra were obtained (a) at the left end of the HB ($N = 1$), (b) at the apex between the HB and the NB ($N = 45$) and (c) around the bottom of the NB ($N = 66$). The middle and the lower panels show the residuals from the best-fit conventional model and from the best-fit new model, respectively.

(NB) N is from 50 to about 65. The data with $N > 65$ belong to the flaring branch (FB). The flux of the disk component gradually increases from the HB to the end of the NB and it seems to saturate during the FB. The inner disk temperature gradually decreases during the NB. The inner disk radius and the radial-temperature gradient, q , continuously increase from the HB to the FB via the NB, although there are large scattering in the FB. The flux of the blackbody component is roughly constant in the HB, and it suddenly decreases during the NB toward the FB. In the FB the flux is roughly constant. This flux evolution of the blackbody component is mainly due to the decrease of the radius during the NB. All of the data can be fitted well with the χ^2 values of less than 2.5. Here, we have to note that Hasinger et al. (1990) used the energy range 1.7–23.3 keV, whereas we used it from 1.7–37.1 keV. F -test indicates that introducing the parameter q significantly improves the fittings of about one-third of the data.

Figure 4 shows a correlation between the inner disk radius, $[R_{in}(\cos i)^{1/2}]$ and the radial-temperature-gradient, q , of the disk. Typical error regions of 68% level for two interesting

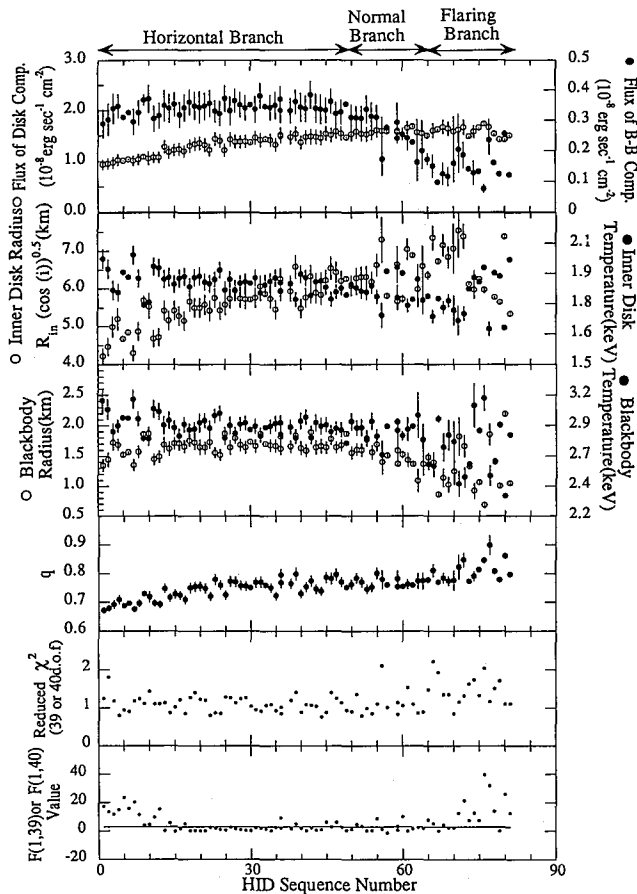


FIG. 3.—Fitting results by the two-component model consisting of the new disk model and a blackbody. The abscissa is the HID sequence number, N . The parameter changes according to the branch behavior can be seen. The bottom panel shows the F values to test the significance of the introduction of the new parameter, q . The fittings of data points above the line plotted in this panel are significantly improved by introducing the new parameter, q , in 90% confidence level. For calculations of inner disk radius, $R_{in}(\cos i)^{1/2}$ where i is an inclination, and the blackbody radius, the distance to Cyg X-2 is assumed to be 8 kpc (Cowley et al. 1979).

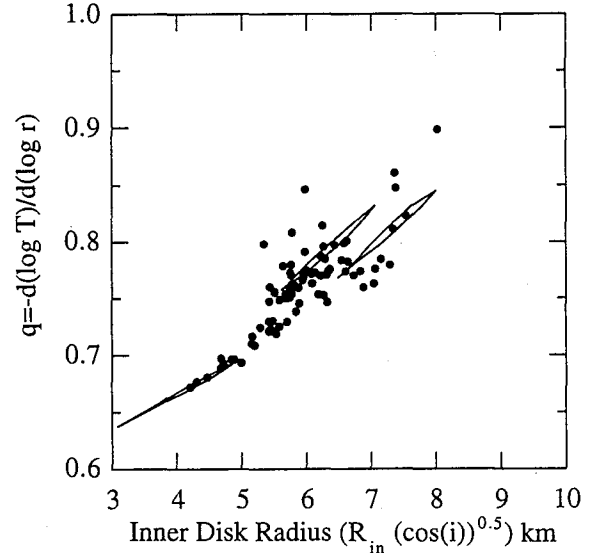


FIG. 4.—Correlation between the radius of inner edge and radial temperature gradient, q , of the disk. Typical 68% error regions for two interesting parameters are plotted for three data points at $N = 1$, $N = 45$, and $N = 66$. Positive correlation can be recognized.

parameters are described for $N = 1$ (left end of the HB), $N = 45$ (apex between the HB and the NB), and $N = 66$ (bottom of the NB). Since the error regions are extremely elongated, the random scattering might become an apparent correlation. However as the inner disk radius $[R_{in}(\cos i)^{1/2}]$ increases from the HB to the FB, q increases significantly. This indicates the positive correlation between them. Figure 5 shows a correlation between $R_{in}(\cos i)^{1/2}$ and the inner disk temperature, (T_{in}) . Again 68% error regions for three typical data are plotted and they show elongated shape. However, significant change of the T_{in} indicates a negative correlation. Note that the $R_{in}(\cos i)^{1/2}$ does not represent a true radius and

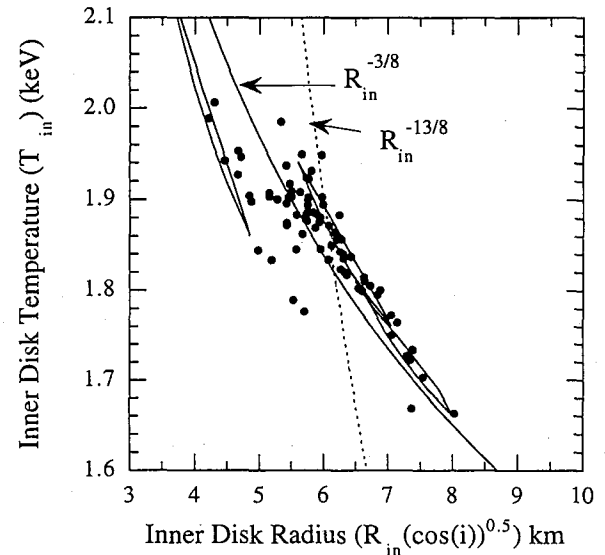


FIG. 5.—Correlation between the radius and the temperature of inner edge of the disk. Typical 68% error regions for two interesting parameters are plotted for three data points at $N = 1$, $N = 45$, and $N = 66$. Negative correlation can be seen. The theoretical dependence of the boundary radius between the gas pressure dominant region and the radiation pressure dominant region ($R_{in}^{-3/8}$) and of the magnetosphere ($R_{in}^{-13/8}$) are plotted.

just a tentative value as mentioned before. This behavior will be discussed in the next section.

4. DISCUSSION

Although Hasinger et al. (1990) discussed the branch behavior based on their results, since they did not specify any models for X-ray emission, the discussion is only qualitative and found no strong constraints for possible accretion-disk structure. Hoshi & Mitsuda (1991) discussed the branch behavior on the basis of the two components model by Mitsuda et al. (1984), in which the X-ray spectra consist of a disk emission and an emission from a neutron star surface, and provided one interpretation for the spectral variation. Honma & Mineshige (1993) discussed the branch behavior using the nonsteady disk model, which is the same as that adopted in the present study, and pointed out a possibility of varying temperature gradients in accordance with the branch behavior. Since only two values extracted from the detailed energy spectra are used to make the HID and CCD, more careful considerations on the emergent spectra must be needed to clarify the emission mechanism of the bright low-mass X-ray binaries. We adopt one particular model (emissions from the accretion disk with a variable radial-temperature-gradient and from the neutron star surface) for the X-ray emission mechanism. As a result, we could obtain quantitative changes of the model parameters in the course of branch transitions. Thus we can firstly discuss the emission mechanism according to the branches though it is based on one specific emission model.

The derived parameters are schematically shown in Figure 6, as well as the other characteristics obtained by the simultaneous observations of radio, optical and ultraviolet. (Hasinger et al. 1990; van Paradijs et al. 1990; Vrtilek et al. 1990). We see that UV flux (Vrtilek et al. 1990) and optical emission lines (van Paradijs et al. 1990) increase from the HB to the FB. It was reported that strong nonthermal radio flares were observed on the HB and on the upper NB but the radio activity was quiet in the lower NB and the FB.

Branch	HB	NB	FB
Radial Temperature Gradient (q)			
Inner Disk Temperature (T_{in})			
Inner Disk Radius (R_{in})			
Black Body Radius (R_{bb})			
Black Body Temperature (T_{bb})			
Fe Absorption Feature			
L_{bb}			
L_{disk}			
UV (flux) and Optical (flux and emission line)			
Radio			
$f(QPO)$			
LFN			
Power spectral shape of X-ray time variation above 0.1 Hz	Flat Top	Power law	Power Law

FIG. 6.—Schematic behavior of the parameters according to the branch behavior. The other characteristics, obtained by the simultaneous observation by radio, optical and ultraviolet, are also shown (Hasinger et al. 1990; Hjellming et al. 1990; van Paradijs et al. 1990; Vrtilek et al. 1990).

The results of the fitting basically agree with those of Hoshi & Mitsuda (1991), except for interesting behavior of the new parameter, q . In their results, the NB is ascribed by the decrease of the blackbody radius from the HB to the FB, while the other parameters remain to be stable. This is consistent with our results, although our results indicates small changes in other parameters. On the HB toward the NB, in contrast, we find some discrepancies: Hoshi & Mitsuda (1991) claimed that T_{in} increases and the ratio of the blackbody luminosity to the disk luminosity decreases, while our results rather suggest that T_{in} is constant, but R_{in} increases, although the behavior of the luminosity ratio is consistent with each other. This discrepancy might arise because of an introduced new parameter, q . For the FB, Hoshi & Asaoka (1993) investigated the behavior of GX 17+2 and suggested that both the R_{bb} and T_{bb} increase from the HB to the end of the FB. Our results, however, show no such clear tendency and indicate highly variable behavior. It should be noted that the behaviors in the FB of Cyg X-2 and GX 17+2 are different from each other on the HID. Cyg X-2 shows the intensity decreases from the bottom of the NB to the FB, whereas GX 17+2 shows the increase. Thus the behavior of the FB might be not common in the Z-sources.

The most important fact concerning the radial temperature gradient, q , is a significant deviation from the conventional value of $q = \frac{3}{4}$ (e.g., Mitsuda et al. 1984). Moreover, q continuously changes from ~ 0.67 at the end of the HB to ~ 0.85 in the FB. This suggests that the disk structural changes cannot be simply described in terms of two parameters; R_{in} and T_{in} , and that the radial structure of the disk itself undergoes substantial and continuous changes from the HB to the FB. These changes seem to be controlled by one single parameter, since the Z-sources are known to move continuously along the Z-shaped trajectory on a timescale of hours without a sudden jump between distinct branches. The most probable parameter is the mass accretion rate, \dot{M} (Priedhorsky et al. 1986; Hasinger et al. 1990). We have to note, however, that the X-ray intensity may not be proportional to \dot{M} , if the apparent X-ray intensity is modified by some mechanisms, such as the spectral variations, geometrical effect, and the existence of other channels of energy dissipation than via the electromagnetic radiation (Hasinger et al. 1990). We may thus suppose that the branch behavior is controlled by \dot{M} . A next question is then whether \dot{M} increase or decreases from the HB to the FB. In the following, we discuss both of two possibilities.

4.1. Increase of Mass Accretion Rate from HB to FB via NB

Hasinger et al. (1990) suggested that the mass accretion rate is increased from the HB to the FB since UV flux increases along this spectral evolution. In the framework of the standard disk model the radius of the inner edge of the accretion disk is kept constant ($3R_s$; R_s = Schwarzschild radius). However, there might be an optically thin, radiation pressure dominant and hot region in the innermost part of the accretion disk, where no efficient radiation is expected. Then we may regard R_{in} to be a boundary between the gas pressure dominant and radiation pressure dominant regions of the disk. If we further assume that this boundary corresponds to the radius where radiation pressure is comparable to gas pressure in the standard disk model, we have

$$R_{in} \propto \dot{M}^{16/21}. \quad (3)$$

The inner disk radius, hence, increases with an increase of the mass accretion rate, but T_{in} (the inner edge temperature of the gas pressure dominant region) decreases along this evolu-

tion as $T_{\text{in}} \propto R_{\text{in}}^{-3/8}$, because of $T \propto \dot{M}^{2/5} R^{-9/10}$ in the gas pressure dominant region (see eq. [2.16] in Shakura & Sunyaev 1973). This line is plotted in Figure 5 and reasonably fits the data.

Since the obtained inner disk radius is interpreted to correspond to the boundary between the gas pressure dominant region and the radiation pressure dominant region, the effect on the main X-ray emitting region (inner part of the gas pressure dominant region) from the torque-free condition changes as the inner disk radius changes. When the inner disk radius is small, the effect from the torque-free condition is large at the main X-ray emitting region. Thus, smaller radial temperature gradients (q) are expected. When the inner disk radius is large, on the other hand, the q -value tends to approach to 0.75 because of a small effect from the boundary condition at the main X-ray emitting region. Furthermore, if the radiation pressure dominant, hot and optically thin region grows up as a result of increasing \dot{M} , there is a possibility that the hot region heats the radiation from the main X-ray emitting region by inverse-Compton up-scattering and makes q more than 0.75.

The effect by electron scattering also affects q . The color temperature is substantially larger than the effective temperature at the electron scattering dominant region and this effect might be more efficient at the high-temperature or small radii region. Therefore q larger than 0.75 might be expected at the high accretion rate.

Another possibility is a vertical swelling of the inner part of the gas pressure dominant region, where a gradual boundary is considered between the gas pressure dominant region and radiation pressure dominant region. The vertical inflation of the disk results in an apparent increase of the inner disk radius (or the effective area of X-ray emitting region) by a geometrical effect. Since such an inflation will be effective only at small radii, an apparent increase in the radial temperature gradient q can be expected.

Therefore, the obtained behavior of q , R_{in} , and T_{in} (see Figs. 4 and 5) can be qualitatively explained. The decrease of the flux of the blackbody component during the NB can be understood in terms of a scattering out, where the plasma of the optically thin region, which is not spherically symmetric, intercepts and scatters photons, thus attenuating the radiation from the surface of the neutron star. Similar effects are expected if a vertically inflated disk block the radiation from the neutron star (see Hoshi & Mitsuda 1991). When the accretion rate is close to the Eddington limit, the accretion flow may not be stable and the observed parameters should be highly variable showing the FB characteristics. The relatively thick plasma, which is going out as a jet, may contribute to the Fe absorption edge which is observed at the bottom of the NB and on the FB. The remaining problem is the radio behavior. Since the radio flares were observed in the HB, the radio flares should occur during low \dot{M} state. However, we note that the relation between the radio activity and the branch behavior is still poorly understood and may depend on the source; for example GX 5-1 is reported to be radio-active in the NB (Tan et al. 1992). We should await further observations to establish a clear tendency.

4.2. Decrease of Mass Accretion Rate from HB to FB via NB

An alternative possibility is that the mass accretion rate decreases from the HB to the FB via the NB. This scenario may also be possible, if we suppose the presence of magnetic field of $\sim 10^8$ G on the surface of the neutron star. The moderately strong magnetic fields will expel accreting material, thereby forming a magnetosphere around the star. The radius

of the magnetosphere is about 10^6 cm around the $1.4 M_{\odot}$ neutron star for the luminosity of about 10^{38} ergs s^{-1} . If this is the case, R_{in} is determined by the magnetic Alfvén radius:

$$r_A \propto \left(\frac{\mu^4}{2GM\dot{M}^2} \right)^{1/7}, \quad (4)$$

where μ is a dipole magnetic moment, G is a gravitational constant, M is the mass of a compact star and \dot{M} is a mass accretion rate. We see that a decrease of the mass accretion rate by a factor of 4 induces a factor of 1.5 enlargement of the Alfvén radius. The innermost disk temperature also decreases rapidly as $R_{\text{in}}^{-13/8}$, according to the standard disk model. This line is plotted in Figure 5 but is steeper than the observational data. We may note again here that the estimated inner disk temperature and radius shown in Figure 5 may not reflect the actual values, if, for example, the color temperature is largely deviated from the effective temperature (Ebisawa et al. 1991). Since an origin of the variable q is not trivial in this scenario, it should be ascribed to an unknown mechanism.

The behavior of the blackbody component from the neutron star surface can be interpreted as follows; The accreting matter onto a neutron star is confined by the magnetic field line. A large magnetosphere (small \dot{M}) can confine mass accretion-pass to smaller region on the neutron star. Then the radius of the blackbody component decreases from the HB to the FB. X-ray characteristics of the FB may depend on the inclination and may be unstable, because of the small emission region. This is consistent with the observations (Shultz et al. 1989). The Fe absorption feature may be seen when \dot{M} is low, since a magnetosphere intercepts the line of sight. Furthermore, in the low-mass binary, the alignment between the rotation axis and the axis of magnetic dipole moment can be expected and no pulsation may be detected.

In this model, radio flares occur during the high mass accretion rate, however, the UV flux behavior, which is bright in the FB, is difficult to explain. Furthermore, this model conflicts with the beat frequency model (Alpar & Shaham 1985; Lamb et al. 1985) for high-frequency QPOs, since it predicts that \dot{M} increases from the HB to the FB.

5. CONCLUSION

We applied a new disk model with a free parameter of $q = -d(\log T)/d(\log r)$ to the X-ray spectra of Cyg X-2. A two-component model consisting of the nonstandard disk and a blackbody radiating neutron star can reasonably fit the data in the range 1.7–37.1 keV, except for the spectra at the bottom of the NB and in the FB, where an absorption edge feature around 8 keV by Fe ions is required with the column density of order of 10^{19} cm^{-2} . Generally speaking, the fitting has been greatly improved by the inclusion of the new parameter q , and the derived q -value significantly deviates from the canonical value of $q = 0.75$ for about one-third of the data. Furthermore, we find that the radial temperature gradient, q , positively correlates with the inner disk radius, R_{in} . This behavior can be interpreted as the change of the effect by the inner boundary condition on the acting torque and also the effect of the Compton scattering by a hot plasma. The temperature decrease with an increase of the inner disk radius can be expected qualitatively from the interpretation that the inner disk radius is determined by the boundary between the gas pressure dominant region and the radiation pressure dominant region. In view of these arguments, we conclude that \dot{M} should increase from HB to the FB via the NB. Another interpretation

is possible, in which an increase of q is due to a vertical inflation of the inner portions of the disk, and/or the radial dependence on the ratio between the color temperature and the effective temperature. We also examined the magnetospheric model, which requires \dot{M} to increase in the opposite direction; i.e., from the FB to the HB. However, many problems still remain for the magnetospheric model.

In conclusion, the improvement of the fitting indicates a justification of introducing q and the introducing q leads to new insights of the accretion disk structure.

The authors would like to thank Professors R. Hoshi, S. Miyamoto, K. Mitsuda and Mr. Y. Kamado for invaluable comments. They also wish to express thanks to the other members of the *Ginga* team, as well as the launching staffs in the Institute of Space and Astronautical Science. This work is supported in part by a Scientific Research Grant from the Ministry of Education, Science, and Culture (No. 05242213, 05836017; S. M.), and by the Yamada Science Foundation (S. K., S. M.).

REFERENCES

- Alpar, M. A., & Shaham, J. 1985, *Nature*, 316, 239
 Cowley, A. P., Crampton, D., & Hutchings, J. B. 1979, *ApJ*, 231, 539
 Czerny, B., Czerny, M., & Grindlay, J. E. 1986, *ApJ*, 311, 241
 Ebisawa, K., Mitsuda, K., & Hanawa, T. 1991, *ApJ*, 367, 213
 Ebisuzaki, T., & Nakamura, N. 1988, *ApJ*, 328, 251
 Hanawa, T. 1989, *ApJ*, 341, 948
 Hasinger, G. 1987, *A&A*, 186, 153
 Hasinger, G., & van der Klis, M. 1989, *A&A*, 225, 79
 Hasinger, G., van der Klis, M., Ebisawa, K., Dotani, T., & Mitsuda, K. 1990, *A&A*, 235, 131
 Hjellming, R. M., Han, X. H., Cordova, F. A., & Hasinger, G. 1990, *A&A*, 235, 147
 Homma, F., & Mineshige, S. 1993, *PASJ*, 45, 201
 Hoshi, R., & Asaoka, I. 1993, *PASJ*, 45, 567
 Hoshi, R., & Mitsuda, K. 1991, *PASJ*, 43, 485
 Kitamoto, S., Tsunemi, H., & Roussel-Dupre, D. 1992, *ApJ*, 391, 220, 227
 Lamb, F. K., Shibazaki, N., Alpar, M. A., & Shaham, J. 1985, *Nature*, 317, 681
 Makino, F., & the Astro-C Team. 1987, *Astrophys. Lett.*, 25, 223
 Mineshige, S., Hirano, A., Kitamoto, S., Yamada, T. T., & Fukue, J. 1994a, *ApJ*, 426, 308
 Mineshige, F., Honma, S., Hirano, A., Kitamoto, S., Yamada, T. T., & Fukue, J. 1994b, in *Theory of Accretion Disks-2*, ed. W. J. Duschel et al. (Dordrecht: Kluwer), 187
 Mitsuda, K., et al. 1984, *PASJ*, 36, 741
 Mitsuda, K., & Dotani, T. 1989, *PASJ*, 41, 557
 Priedhorsky, W., Hasinger, G., Lewin, W. H. G., Middleditch, J., Parmar, A., Stella, L., & White, N. E. 1986, *ApJ*, 306, L91
 Sanbuichi, K., Yamada, T. T., & Fukue, J. 1993, *PASJ*, 45, 443
 Schultz, N. S., Hasinger, G., & Trümper, J. 1989, *A&A*, 225, 48
 Shakura, N. I., & Sunyaev, R. A. 1973, *A&A*, 24, 337
 Sunyaev, R. A., & Titarchuk, L. G. 1980, *A&A*, 86, 121
 Tan, J., Lewin, W. H. G., Hjellming, R. M., Penninx, J., van Paradijs, J., van der Klis, M., & Mitsuda, K. 1992, *ApJ*, 385, 314
 Turner, M. J. L., et al. 1989, *PASJ*, 41, 345
 van Paradijs, J., et al. 1990, *A&A*, 235, 156
 Vrtillek, S. D., Raymond, J. C., Garcia, M. R., Verbunt, F., Hasinger, G., & Kurster, M. 1990, *A&A*, 235, 162
 White, N. E., Peacock, A., & Taylor, B. G. 1985, *ApJ*, 296, 475
 White, N. E., Stella, L., & Parmar, A. N. 1988, *ApJ*, 324, 363
 You, J. H., Lu, T., Wei, C. Y., & Wang, T. G. 1992, *ApJ*, 394, 283